Terra Antartica
1998, **5**(3), 327-335

CRP-1 Fracture Arrays: Constraints on the Neogene-Quaternary Stress Regime along the Transantarctic Mountains Front, Antarctica

T.J. WILSON & T.S. PAULSEN

Byrd Polar Research Center / Dept. of Geological Sciences, Ohio State University, Columbus, OH, 43210 - USA

Received 15 July 1998; *accepted in revised form* 13 October 1998

Abstract - Fractures in core of Quaternary-Miocene age recovered at Cape Roberts Project drillsite (CRP-1) were analysed to document the past and present stress regime along the Transantarctic Mountains Front. We identified both natural and induced fractures in the CRP-1 core. Natural fractures include microfaults, clastic dykes, and shear fractures. Induced fractures created by the drilling or coring process include petal and petal-centreline fractures, disc fractures, and subhorizontal fractures that formed due to the influence of sea swell on the drilling. Natural fracture sets document a normal-faulting type stress regime, with a vertical maximum principal stress. Petal and petal-centreline fractures in palaeomagnetically orientated core intervals show that the contemporary maximum horizontal stress is orientated north-northeast to south-southwest in the Cape Roberts region. Collectively, the natural and induced fractures document a stress regime that is compatible with regional late Cenozoic dextral transtension along the Transantarctic Mountains Front, consistent with previous interpretations of both onshore and offshore structural records.

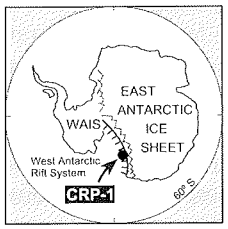

INTRODUCTION

The Cape Roberts Project drillsite (CRP-1) lies along the Transantarctic Mountains Front, which separates the uplifted Transantarctic Mountains from the Victoria Land rift basin of the West Antarctic rift system. Faulting along the Transantarctic Mountains Front has been interpreted to accommodate the large differential relief between the mountains and the rift basin, and this fault zone has been compared with the normal border fault systems that bound rift basins in the East African rift system (Tessensohn & Wörner, 1991; Davey & Brancolini, 1995). The Transantarctic Mountains Front has a long history of Mesozoic-Cenozoic rift-related displacements, with early, presumably mainly normal-sense displacements apparently followed in the Cenozoic Era by rift-related transtensional deformation (Wilson, 1992, 1995; Salvini et al., 1997). The study of fractures found within the CRP-1 core provides the first opportunity to obtain a well-dated kinematic and dynamic structural record along the Transantarctic Mountains Front.

Brittle fractures form by instantaneous rupture when the applied stress exceeds the material strength. The orientation of the principal stresses that produce the rupture plane can be reconstructed if the fracture orientation and the mode of failure (extension, shear) can be documented. Natural fractures, which are present in the rock prior to drilling, generally yield information on the palaeostress regime. Natural neotectonic fractures, younger than ~2 Ma, may record the contemporary stress regime and are typically found in near-surface portions of core (Evans, 1994; Engelder, 1987). If natural fracture arrays with different orientations are present in strata of different ages in a sequence, then changes in the orientation of the principal stresses can be reconstructed with respect to time (Kleinspehn et al., 1989; Evans, 1994; Teyssier et al., 1995), provided that age-controlled changes are differentiated from changes resulting from contrasting mechanical properties of layers. A primary objective of this ongoing study is to identify fracture sets of different ages within the cored rift sequence in order to test models for changing kinematics along the Transantarctic Mountains Front. Another objective is to identify induced fractures that formed in response to drilling- or coring-related perturbations of the ambient stress field. The orientations of induced fractures are commonly controlled, at least in part, by the *in situ* stresses acting on a rock body (*e.g.*, Plumb & Cox, 1987; Kulander et al., 1990), and thus provide a means of obtaining contemporary horizontal stress directions at the Cape Roberts drillsite.

CRP-1 DRILLING

The Cape Roberts Project utilized a drill rig located on fast sea ice over a water depth of ~150 m. Unlike typical drilling operations, the sea-ice drilling platform experienced vertical motion due to tides and to sea swell in the Ross Sea. Although the orientation of the drill hole was not directly measured, it is estimated to be within about $\pm 2^{\circ}$ of vertical. The drilling programme obtained 147 m of core prior to the storm-related termination of drilling. The upper portion of the core consists of ~43 m of compacted but unconsolidated and uncemented Quaternary strata, and the lower portion consists of semi- to moderately-lithified and uncemented strata of Miocene age. Diamictite,

sandstone, siltstone, and their unlithified equivalents are the dominant core lithologies, almost all interpreted to be glacigenic (Cape Roberts Science Team, 1998).

FRACTURE STUDY PROCEDURES

All fractures in the CRP-1 core were logged during examination of the whole core. We noted and described fracture morphology, any fracture surface features, fracture terminations, cross-cutting and abutting relations. Fracture attitudes (dip and dip direction) were measured with respect to an arbitrary north defined by a red line scribed along the length of the core. We also used DMT's Corelog® software to digitise structures on 'unrolled' whole-core scans and to produce logs of fracture attitude and type *vs* depth. These logs were used to check hand-measured orientations and to identify additional, handling-induced fracture planes. We planned to orientate the core, and thus the fractures, by using a down-hole core-orientating tool between core runs and by comparing orientated borehole televiewer logs of the borehole wall with 'unrolled' whole core scans. The instability of the borehole and the early termination of drilling precluded use of these methods. Limited portions of the core were reorientated using palaeomagnetic data (Paulsen & Wilson, this volume), but most of the core could not be reorientated due to a lack of sufficient data.

We grouped fractures into sets based primarily on morphology and divided some sets into subgroups based on dip angle. These characteristics, together with any fractographic features, were used to assign fractures to 'natural' or 'induced' categories wherever possible. For core intervals that were palaeomagnetically reorientated (Paulsen & Wilson, this volume), fracture attitudes were analysed stereographically to further delineate fracture sets. For each set we calculated the number of fractures per metre length of core to construct histograms of fracture occurrence *vs* depth (Fig. 1). Because lithological boundaries, sequence boundaries and breccia intervals commonly occur with spacing well over 1 metre, this simple calculation is adequate to compare these features with fracture density determined in this way.

INTERPRETATION OF FRACTURE MODE OF ORIGIN

Criteria used for distinguishing natural and induced fractures are detailed in Kulander et al. (1990). Features that are diagnostic of natural fractures include mineralisation, alteration, well developed slickenside surfaces, offset and flexure of bedding planes, and cataclastic shear-band textures. Geometric arguments for inferring fractures of probable natural origin include parallelism with fractures associated with one of the diagnostic features cited above, and shear fracture orientations compatible with those predicted by Anderson's (1951) theory of faulting in typical crustal stress regimes. Some types of induced fractures have distinctive geometries that have been shown by modelling to mimic drilling-induced stress trajectories (Lorenz et al., 1990; Li & Schmitt, 1997). Other criteria used to recognise drilling-, coring- and handling-induced fractures include the presence of a fracture origin point on the fracture surface, hackle plume and arrest line patterns related to core geometry, abrupt changes in fracture geometry at core margins ('hooking') or at other fractures within the core, all indicating that the fracture initiated and propagated within the core.

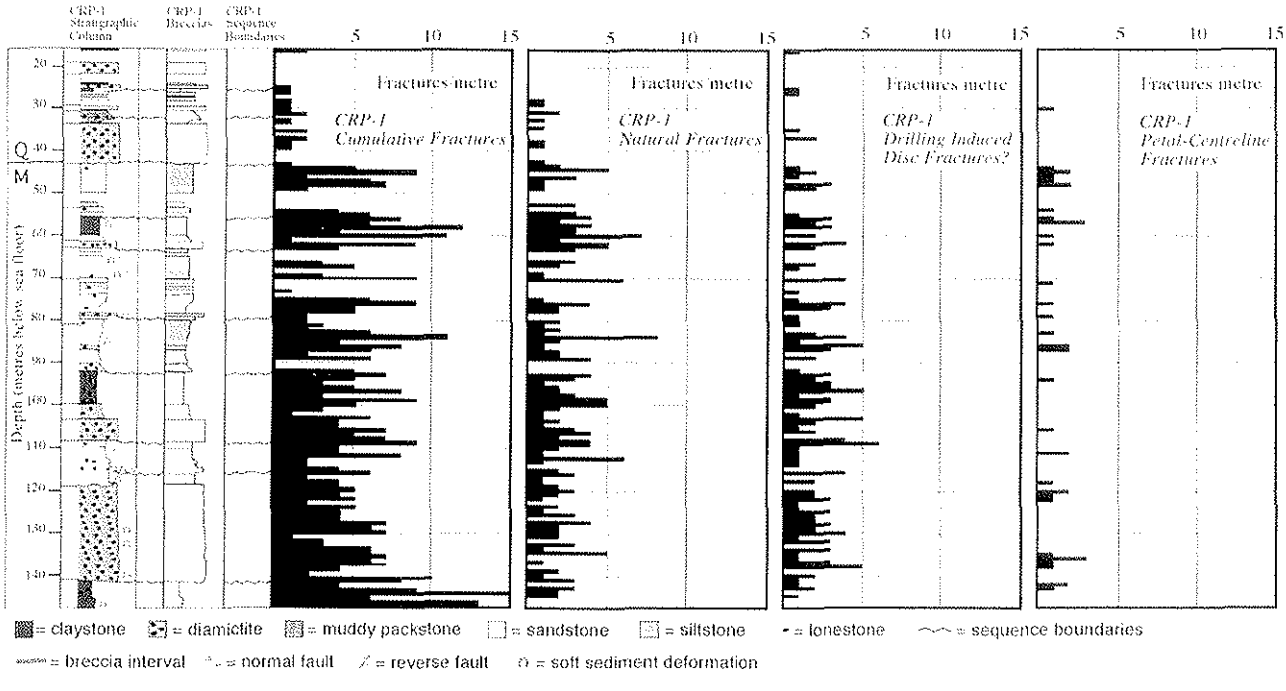

Fig. 1 - Fracture density plot showing the number of cumulative, natural, disc, and petal/petal-centreline fractures per metre of core with relation to age, depth, lithology, breccia intervals, and sequence boundaries within the CRP-1 core.

Most of the fractures in the CRP-1 core lacked surface fractographic features. This is probably because the strata are poorly indurated, since delicate surface features are best developed in highly indurated, fine-grained materials (*e.g.*, Kulander et al., 1979). We have used the sparse fractographic record, together with geometric arguments, to interpret fracture origin; ambiguities are noted in the descriptions that follow. In the case of natural fractures, fracture mode (extension, shear) must also be known in order to infer stress patterns. Fracture mode is not well constrained from the core observations, due to the paucity of surface features. However, geometric arguments based on orientations predicted for natural shear fractures, and on known structural aspects of the regional setting, suggest possible fracture mode interpretations. These interpretations, and the stress interpretations we derive from them, can be tested by recovery and analysis of more complete fracture data sets from orientated core obtained during the next drilling season.

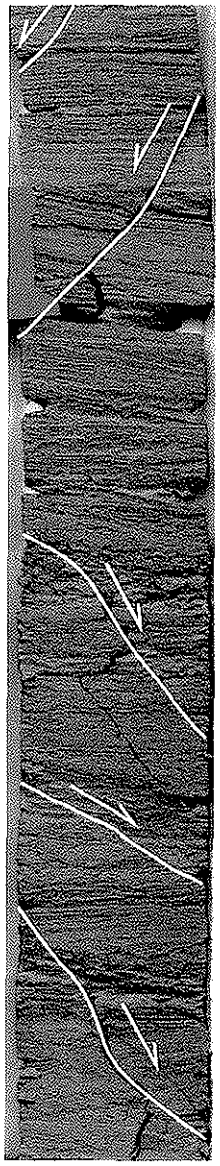

Fig. 2 - Corescan® image of conjugate normal microfaults within laminated sandstone in slabbed CRP-1 core at 66 mbsf. Horizontal width of core is 6.1 cm.

NATURAL FRACTURES

Microfaults

In the 150 m of CRP-1 core, we identified 6 definite microfaults with dip separations of bedding of 2-6 mm. Faults have dips that range from 55 to 70° and have curved, listric profiles. A conjugate set of microfaults with normal-sense offset of bedding occurs in an interval of laminated sandstone between 65-70 metres below sea floor (mbsf) (Fig. 2). Another normal-sense microfault occurs at 115.97 mbsf. This fault occurs in a section of orientated core; it has a north-northeast strike and dips northwest (Fig. 3). One microfault with reverse-sense displacement occurs at 109.12 mbsf.

Clastic Dykes

Clastic dykes occur in the core at 133.30 and 139.05 mbsf. The dykes occur within diamictite, are composed of sand, have planar, sharp boundaries, and have thicknesses of approximately 1-2 cm. Both dykes dip at 77°. One dyke occurs in orientated core; it strikes northeast and dips southeast (Fig. 3). Small, discontinuous,

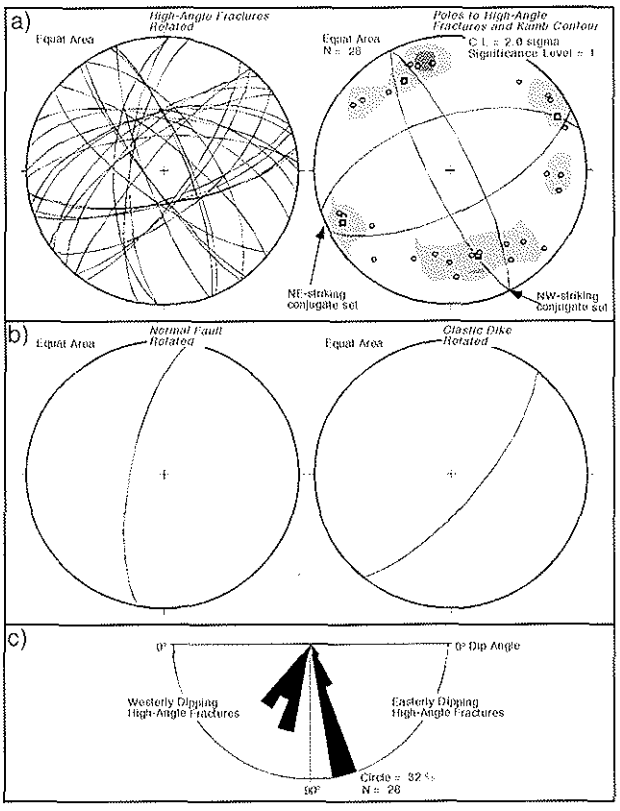

Fig. 3- Stereoplots showing the orientations of high-angle (Group 1H) natural fractures within orientated core intervals. *a)* Great-circle stereoplot and Kamb contour plot of poles to high-angle, natural fracture planes. Note the fracture planes form sets with similar strikes and equal but opposite dips, typical of conjugate shear fractures. *b)* Great-circle stereoplots showing a north-northeast-trending normal fault and a northeast-trending clastic dyke from orientated core intervals. *c)* Rose-diagram plot showing westerly and easterly dipping high-angle fractures, which shows a dip distribution expected for conjugate normal shear fracture sets.

irregular fractures associated with breccias in the core also have a fill of fine clastic material (Passchier et al., this volume).

Fracture Sets

Interpretation as Natural Fractures

Fractures with dips between ~30 and 80 degrees are common in the CRP-1 core and are referred to below as Group 1 fractures. Planar fractures with such dips are atypical of fractures induced by drilling-, coring-, or handling-related stresses. Rather, dips in this range are typical of shear fractures formed by common crustal stress configurations (Anderson, 1951). There is some evidence suggesting that Group 1 fractures were present prior to coring. Drilling operations were frequently impeded by jamming of core entering the core barrel, indicating that numerous fractures were present in the rock prior to coring. Several of these fractures also have short, discontinuous striae orientated approximately down the dip of the fracture plane (Fig. 4). The presence of striae is compatible with either a shear fracture (fault) origin for the fracture or, given the relatively soft state of the sediment, with shear induced on an existing fracture when the core was forced upward into the core barrel. Several Group 1 fractures had abundant drilling mud coating their surfaces, indicating that they were present prior to entry into the core barrel. Some Group 1 fractures were associated with broken, rubble zones where core material was apparently damaged by drilling. A portion of Group 1 fractures had other fractures terminate against them, including some induced fractures, indicating that they formed earlier than at least some other core fractures. However, some Group 1 fractures terminated within the core, indicating an induced origin. An induced origin for some Group 1 fractures, but not others, could be due to propagation of pre-existing natural microfractures due to coring- or handling-induced stresses. We observed the formation of handling-induced fractures parallel, and in proximity, to moderately-dipping existing fractures in a few cases.

Based on the evidence that Group 1 fractures were present prior to drilling, their apparent incompatibility with induced fracture geometries, and their compatibility with natural fracture geometries, we interpret this set of fractures as natural fractures. In figure 1 we show the density (fractures/m of core) of these inferred natural fractures within the CRP-1 core. Although the highest fracture densities occur in finer-grained material, there is no systematic correlation between lithology and fracture abundance (Fig. 1). Fracture tips were typically not present in the core, thus the data do not constrain whether fractures are confined to discrete beds or lithologic units. There is an overall increase in fracture abundance across the Quaternary/Miocene contact (43.10 mbsf; revised boundary, Fielding et al., this volume), consistent with the increased induration and the longer history of the Miocene strata. However, the overall poor-to-moderate lithification and lack of cementation of CRP-1 strata suggest that layering probably did not exert a strong influence on fracturing.

Both fractures and breccias are particularly abundant in the uppermost Miocene strata, but elsewhere in the core there is no consistent correlation between increased fracture abundance and the presence of brecciated intervals (Fig. 1). Miocene diamictites at ~63, 79, 123 and 134 mbsf show microstructural evidence of subglacial shear (van der Meer, this volume); the upper two diamictite horizons correlate with high fracture abundance, whereas the lower two do not.

Interpretation of Fracture Mode

Group 1 fractures were subdivided into a subgroup of fractures with dips between 26 and 50 degrees (Group 1L) and a second subgroup with dips between 51 and 80 degrees (Group 1H) (Fig. 5). We chose these dip intervals

Fig. 4 - Photograph of a high-angle fracture with down-dip striae in the CRP-1 core. Core is 6.1 cm in diameter.

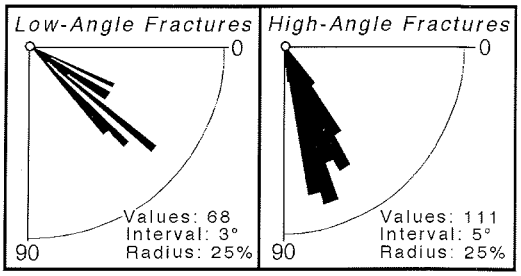

Fig. 5 - Rose-diagram plots showing the dip-angle distribution of low-angle (Group 1L) and high-angle (Group 1H) natural fracture subgroups within the CRP-1 core.

because the 'low-angle' (1L) group represents a typical range of dips for thrust-sense shear fractures and the 'high-angle' (1H) group represents a typical range of dips for normal-sense shear fractures (Anderson, 1951).

The high-angle fracture group (1H) has dips equivalent to the dips of microfaults in the core, most of which are normal faults (Fig. 6). Dips of approximately 60 degrees are typical of normal-slip faults and Group 1H fractures have dips that cluster around that dip range (Fig. 5). Five of seven fractures with down-dip striae (Fig. 4) fall in this geometric group. In the core intervals that could be orientated, the fracture planes form sets with similar strikes and equal but opposite dips, typical of conjugate shear fractures (Fig. 3). The clastic dyke and normal microfault that occur in orientated core have northeasterly strikes, similar to the northeast-striking conjugate fracture set (Fig. 3). No origin points or hackle plume features indicative of extension were observed on the high-angle fractures although, of course, these features were rare overall. Most joint sets, generally taken to be opening-mode extension fractures, have subvertical orientations, whereas dip-slip shear fractures typically have dips ranging from 30 to 75° (Engelder, 1987). Taken together, the available evidence suggests that the Group 1H fracture set formed as natural, conjugate shear fractures with a subvertical σ_1.

The low-angle fracture group (1L) remains enigmatic. Two low-angle fractures had striae on their surfaces, indicating shear, but no shear-sense indicators. Several Group 1L fractures had possible hackle or origin points indicative of extension, but most had no surface features. The tectonic rift-related setting of the region does not predict thrust faulting. If the Group 1L fractures represent thrust-sense microfaults of tectonic origin, they must have formed where local compression occurred, perhaps at a fault jog or transverse accommodation structure along the rift margin. Alternatively, thrust-sense microfaults could have formed as a result of glaciotectonism. The low-angle dips of these fractures are compatible with families of microshears (*e.g.*, Riedel shears) formed as a reult of subhorizontal shear, and thus are consistent with a subglacial shear origin (*e.g.*, van der Wateren, 1995). Group 1L fractures are abundant in proximity to the levels of inferred subglacial shear at *c.* 63 and 79 mbsf (van der Meer, this volume), suggesting a genetic relation. A third alternative is that Group 1L fractures originated as steeper normal-sense microfaults that were later rotated to shallower dip angles during compaction of the sedimentary strata. If this is the case, Group 1L fractures should be older than the steeply dipping 1H fractures, but sparse cros-scutting relations are ambiguous. Features associated with fracture rotation due to compaction, such as curvature or indentation of fractures around rigid glacigenic lonestones in the diamictites, were not observed in the CRP-1 core.

Low-angle fractures in the orientated portions of the core have orientations that are more scattered than the high-angle natural fractures, but appear to define 3-4 diffuse subsets (Fig. 7). Though not clearly defined, the fracture pattern hints at 2 conjugate fracture sets, resembling fault systems with orthorhombic symmetry typical of triaxial strain (Reches, 1978; Krantz, 1988). If so, the low-angle fracture sets may represent rotated normal-sense shear fractures that formed with a vertical σ_1. However, if the low-angle fractures do not comprise two conjugate sets, they probably did not form as a result of tectonism, unless fractures formed at different times under different stress conditions. Such rapid changes in the stress field seem unlikely in the short interval of time represented by the strata. On the other hand, different fracture orientations at different levels would be expected if these fractures originated by glaciotectonism, since ice motions and related shear directions would most likely differ between glacial cycles.

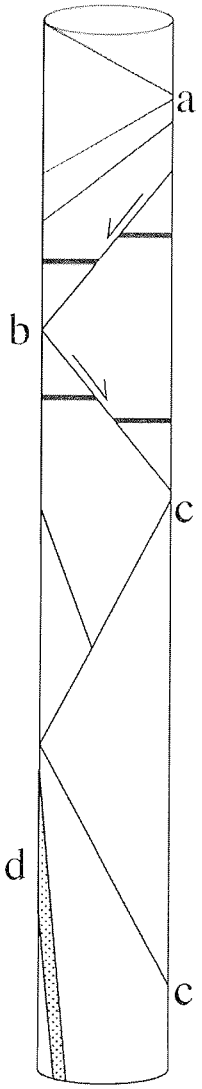

Fig. 6 - Schematic diagram showing typical geometries of interpreted natural fractures in the CRP-1 core.
a = Low-angle (26°-50°) shear? fractures;
b = conjugate, high-angle (51°-80°) normal microfaults;
c = conjugate, high-angle (51°-80°) shear fractures;
d = high-angle clastic dyke.

INDUCED FRACTURES

Disc Fractures

Disc fractures form normal to the axis of a drillcore in regions of high horizontal stress (Obert & Stephenson, 1965; Dyke, 1989). Subhorizontal to very low-angle (≤25 degree dip) fractures are abundant within CRP-1 core (Fig. 1). One subhorizontal fracture had an origin

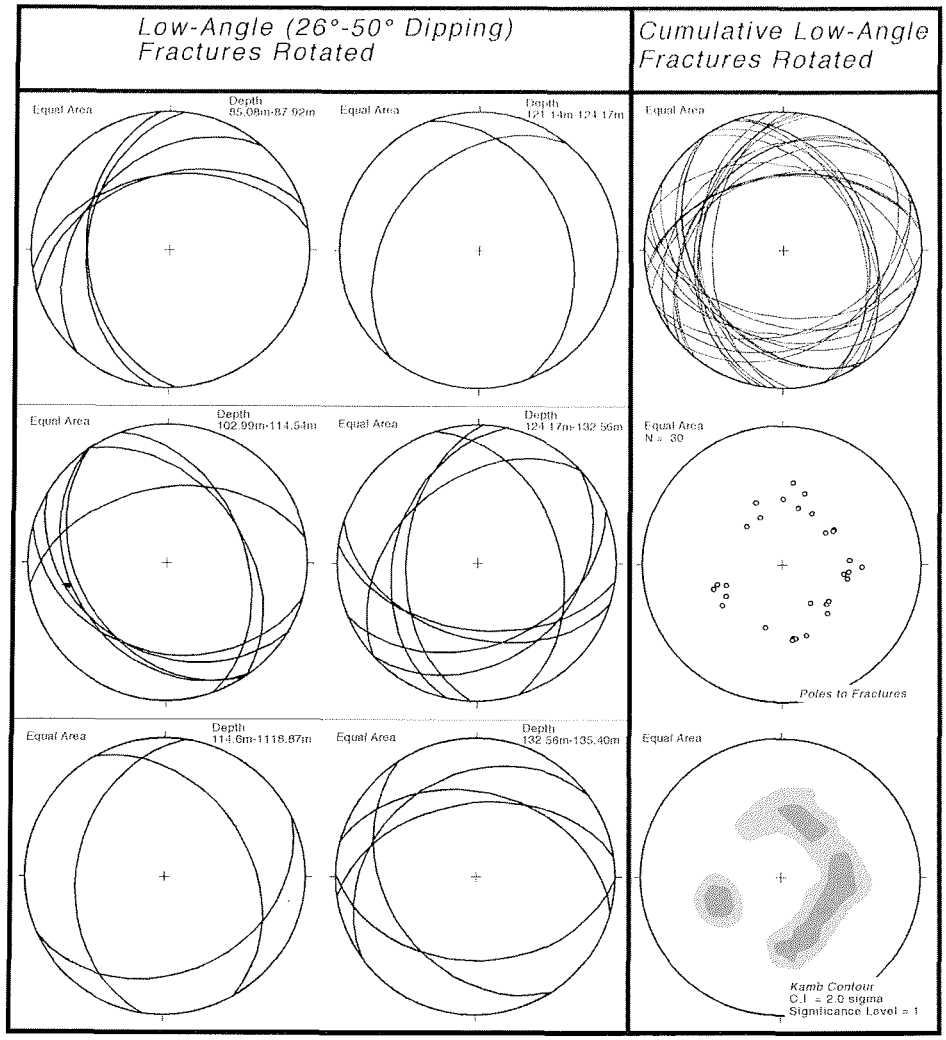

Fig. 7 - Stereoplots showing the orientations of low-angle (Group 1L) natural fractures within orientated core intervals. Note that Group 1L fracture orientations appear to change between depth intervals. For the cumulative data set, note the scatter of orientations and the possible 3 or 4 diffuse fracture groups.

point on the fracture surface indicating nucleation at a lonestone in diamictite (Fig. 8), proving induced, tensile failure. The majority of probable or possible hackle, arrest lines, or origin points, which are indicative of tensile failure, occurred on fracture surfaces of this group. Low-angle fractures followed bedding or cross-laminae in some cases, suggesting failure along pre-existing weaknesses, but most of the cored sequence lacked well-defined bedding. Several fractures of this group were lined with drilling mud or associated with broken rubble zones, compatible either with a natural fracture origin or a drilling- or coring-induced origin, when drilling mud had access to the fracture planes. Given the very low-angle dip of these fractures and the evidence for tensile failure, it is highly probable that a proportion of these fractures represent disc fractures.

Fig. 8 - Photograph of a subhorizontal fracture with an origin point at a pebble and fine hackle on the fracture surface, demonstrating induced, tensile fracture origin. Core is 6.1 cm in diameter.

Petal and Petal-Centreline Fractures

Petal and petal-centreline fractures form in response to stress induced beneath the advancing drill bit, and thus originate outside of the core boundaries and have curved surfaces that follow the induced stress trajectories (Lorenz et al., 1990; Kulander et al., 1990; Li & Schmitt, 1997). Curviplanar fractures that terminate within the core and have the diagnostic curved shape of petal or petal-centreline fractures (Fig. 9) are abundant in the CRP-1 core. These

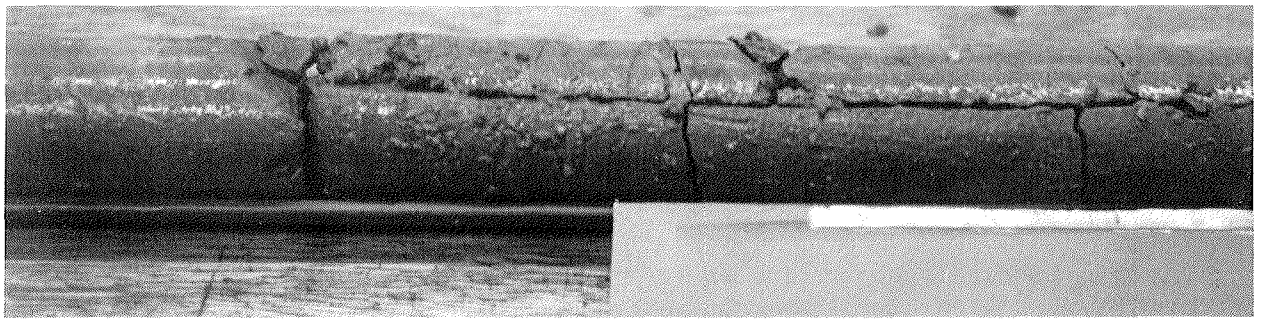

Fig. 9 - Photograph of a petal-centreline fracture in the CRP-1 core at 136 mbsf. Note petal curvature inward and downward from margin and vertical centreline fracture following core axis. The core section is 38 cm long.

fractures occur at 29.65 mbsf within the Quaternary section and throughout the Miocene strata to the base of the CRP-1 core (Fig. 1). One petal-centreline fracture had possible arrest lines on the fracture surface, but otherwise these fractures lacked the distinctive surface plumes and arrest lines reported by Kulander et al. (1990). The majority of the fractures in this set were typical petal fractures, concave downward and terminated toward the core interior, although a few were concave upward, where bedding planes apparently influenced fracture propagation (Fig. 10). Some curved fractures had the form of 'inverted petals' (Fig. 10); however, existing drilling-related stress models do not explain this fracture geometry.

There is no systematic correlation between petal fracture abundance and lithology within the CRP-1 core (Fig. 1). Changes in petal fracture density down core were more likely to be related to the drilling operations, since petal fractures initiate in response to an increase in bit stress caused, for example, when the driller releases the draw works, resulting in a sudden increase of the weight on the bit (Lorenz et al., 1990). Such changes in weight on the bit apparently occurred during CRP-1 drilling due to the rise and fall of the drill rig when the sea ice platform was affected by sea swell. This mechanism explains the increase in petal fracture abundance near the base of the cored interval, which was obtained when there was significant sea-ice motion during a major storm.

Petal and petal-centreline fractures in orientated core intervals form a well-defined north-northeast striking group (Fig. 11). The two approximately east-west fractures in figure 11 were tentatively classified as petal-centreline fractures, based on their steep dips and slightly curviplanar shapes. However, their anomalous orientation with respect to the rest of the petal fractures suggests that they might not belong to the petal group, or that fracture propagation was influenced by a local stress perturbation, such as a pre-existing fracture within the core (Paulsen & Wilson, this volume).

Other Coring- and Handling-Induced Fractures

A population of subhorizontal fractures definitely formed due to vertical motion of the drill string, when the drill-bit rose and 'plucked' a segment of core from the base of the borehole. Subsequent spinning of the core segment as the drill-bit re-engaged created finely etched circular

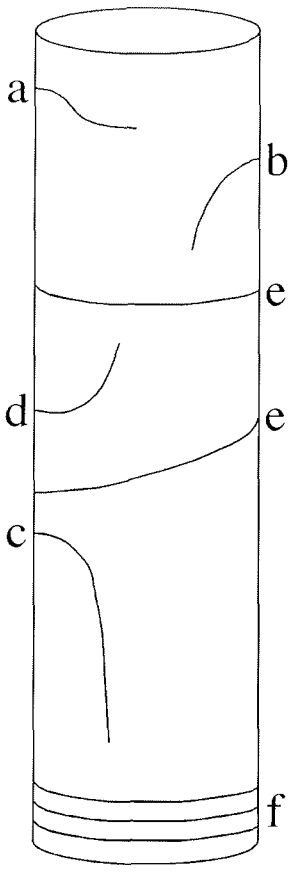

Fig. 10 - Schematic diagram showing typical geometries of interpreted induced fractures in the CRP-1 core.
a = concave upward petal fracture;
b = typical concave downward petal fracture;
c = petal-centreline fracture;
d = possible inverted petal fracture;
e = low-angle disc fractures;
f = subhorizontal 'plucking' fractures formed by vertical drill bit motion due to storm-related sea swell.

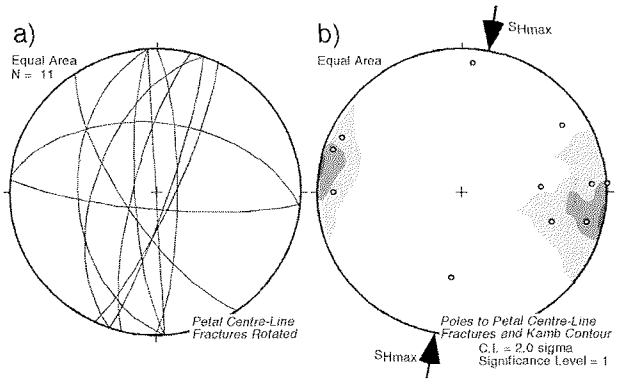

Fig. 11 - Stereoplots showing the orientations of petal/petal-centreline fractures within orientated core intervals. *a)* Great-circle stereoplot and *b)* Kamb-contour plot of poles to fracture planes showing the overall north-northeast-trend of petal/petal-centreline fractures and of S_{Hmax}.

grooves on these fracture surfaces (Cape Roberts Science Team, 1998). These fractures appear at *c.* 140 mbsf, and are increasingly abundant near the base of the core, marking the increased sea swell during the storm that caused early termination of drilling. Some fractures in the core had a cone-shaped morphology similar to torsion fractures described by Kulander et al. (1990), suggesting that they formed by twisting of the core during coring.

Handling-induced fractures also formed within the CRP-1 core, typically in the time interval between initial-core fracture logging and the scanning of the whole-core segments. Most of these fractures had dips of 15 degrees or less, but a few were parallel to more steeply dipping, inferred natural fractures, suggesting they may have nucleated on microfractures in the core and then propagated as a result of handling-related stress. Other handling-induced fractures include axial cracks and various other fractures which formed as the cores were split, and as a result of the collapse of the round core in the flat-bottomed storage boxes as the boxes flexed during transport.

STRESS REGIME OF THE CRP-1 REGION

PALAEOSTRESS REGIME

Stress Orientations

The normal microfaults and the high-angle natural fracture arrays (Group 1H) comprise a conjugate fracture system. Andersonian faulting theory predicts that normal-sense conjugate shear fractures form with the maximum compressive principal stress, σ_1, as the vertical bisector of the acute angle between the conjugate sets, with the intermediate principal stress, σ_2, horizontal and parallel to the line of intersection of the fracture sets, and with the minimum compressive stress, σ_3, horizontal and perpendicular to σ_1 and σ_2. The near-vertical clastic dykes in the core, which represent extension fractures formed parallel to the σ_1 - σ_2 plane and perpendicular to σ_3, are also consistent with this stress regime. The high-angle natural fracture sets in the orientated portion of the core define two conjugate fracture sets which strike northeast and northwest. Both of these conjugate fracture sets occur throughout the core; therefore the two sets cannot be ascribed to a particular core sequence or time interval. We did not observe any clear cross-cutting relations between these two fracture sets to establish their relative age. If they have different ages, the two fracture sets must represent two different stress configurations, with the minimum stress, σ_3, changing from northeast-southwest to northwest-southeast, or *vice versa*, with time. However, if the two fracture sets are coeval, they suggest a non-Andersonian, triaxial regime (*e.g.*, Krantz, 1988; Reches, 1978).

Because the high-angle natural fractures occur throughout the cored Miocene interval, the deformation regime responsible for their development must be younger than ~17.5 Ma, which is the age of the youngest preserved Miocene strata. The fact that a few of the high-angle natural fractures occur in the Quaternary section of the core suggests that the same stress regime persists today.

Tectonic *vs* Glaciotectonic Deformation

A stress regime with vertical maximum compressive stress ($\sigma_1 = \sigma_v$) is characteristic of continental rift regimes and thus CRP-1 fractures may reflect rift-related tectonic deformation within the Cape Roberts region. The northwest and northeast orientation of the high-angle natural fracture sets is approximately coincident with the strikes of offshore faults interpreted from seismic reflection data (Hamilton et al., this volume) and aeromagnetic data (Bozzo et al., 1997), suggesting a genetic relationship and, therefore, a tectonic origin for these fractures.

Given the possibility of repeated glacial overriding of the Cape Roberts site, it is also possible that the natural fractures may have developed in response to a glacial load imposing a vertical compression. The vertical load of an ice mass alone results in an isotropic 'glaciostatic' stress. According to Aber et al. (1989), the stresses responsible for glaciotectonic deformation are dominated by horizontal stress gradients localised near ice margins, where the vertical load, and therefore the resolved horizontal stress component, changes rapidly as the ice thickness diminishes to zero. Basal shear stresses generated by ice motion also contribute to glaciotectonism, but to a smaller degree. In ice-marginal and subglacial shear settings, the maximum stress is horizontal, which predicts a thrust-faulting stress regime, and is expected to be perpendicular to the ice sheet margin (parallel to the direction of most rapid change in ice load). In this scenario, normal faulting would only develop near local perturbations in the stress field caused, for example, by the termination of structures. However, conjugate normal fault sets have been attributed to other processes associated with glaciotectonism, such as loading by subglacial overthrusts (van der Wateren, 1987) or the formation of Riedel shear sets beneath subglacial shear zones (van der Wateren, 1995). We cannot clearly identify this type of setting from the context of the core alone, but the lack of evidence for pervasive shear deformation throughout the sequence argues against extensive glaciotectonic shear. Thus, it seems more likely that the normal-sense microfaults, the clastic dykes and the high-angle natural fracture sets, which are all compatible with a vertical maximum compression direction, formed as a result of rift-related tectonism.

CONTEMPORARY STRESS REGIME

Systematic comparison of the orientation of petal-centreline fractures and other *in situ* stress orientation indicators have shown that the strikes of these fractures parallel the regional maximum horizontal stress direction (Plumb & Cox, 1987; Lorenz et. al., 1990). Petal-centreline fractures are extension fractures that form perpendicular to σ_3, and follow the σ_1-σ_2 plane, where σ_1 is equal to the overburden stress plus the stress from the weight on the drill bit and σ_2 is the maximum *in situ* horizontal stress (Lorenz et al., 1990). The petal-centreline fractures in the CRP-1 core occur in both Quaternary and Miocene strata and are clearly neotectonic, induced fractures. Petal-centreline fractures in orientated core intervals indicate a north-northeast to south-southwest orientation for the

maximum horizontal contemporary stress and, perpendicular to it, a west-northwest to east-southeast minimum horizontal contemporary stress in the Cape Roberts region (Fig. 11).

The contemporary stress orientations that we interpret from the petal-centreline fractures are compatible with the single orientated normal microfault and clastic dyke, and together these structures indicate a normal-faulting regime with the maximum horizontal stress equal to σ_2 and a vertical σ_1 maximum compressive stress. This stress regime is broadly compatible with the northeast-striking, conjugate, high-angle natural fracture set. Either the northwest-striking natural fracture set is older, or, if the high-angle conjugate natural fracture sets are coeval, then they must have formed in a triaxial strain regime.

A normal-fault stress regime fits the rift tectonic setting predicted for the margin of the Victoria Land rift basin. The north-northeast to south-southwest maximum horizontal stress is oblique, however, to the northwesterly trend of the Transantarctic Mountains Front structural boundary, and thus predicts a component of right-lateral displacement along the Transantarctic Mountains Front. Wilson (1995) documented brittle faults with north to northeast trends in bedrock at Cape Roberts and along the coastal margin of the Transantarctic Mountains in the McMurdo Sound region. Slip directions on these faults indicate an early normal dip-slip episode, followed by a younger, dextral oblique- to strike-slip episode, both of which are interpreted to be the result of dextral transtensional rifting during the Cenozoic Era. The Neogene-Quaternary stress regime documented here is consistent with dextral transtensional kinematics, suggesting that the motions recorded in the uplifted mountain block along the Transantarctic Mountains Front may have continued through late Cenozoic time, and possibly continue today.

ACKNOWLEDGEMENTS

This work was funded by NSF grant OPP-9527394 to T.J. Wilson. Timothy Paulsen was partially supported by the Byrd Postdoctoral Fellowship, Byrd Polar Research Center, Ohio State University. Discussion with Byron Kulander helped us to plan the core fracture study. We thank Christie Demosthenous for help in producing the figures and Rick Allmendinger for stereonet programs that greatly simplified our data analysis. Dr. G. Rafat generously volunteered his time and expertise for set up and training on the CoreScan®. Fee waivers and software access provided by DMT facilitated this research. We thank Mark Fischer for comments which helped us to improve the clarity of this paper.

REFERENCES

Aber J.S., Croot D.G. & Fenton M.M., 1989. Glaciotectonic landforms and structures. In: Bentley C.R. (ed.), *Glaciology and Quaternary Geology*, Kluwer Acad. Publ., Dordrecht, Netherlands.

Anderson E.M., 1951. *The Dynamics of Faulting*. Oliver & Boyd, Edinburgh, 206 p.

Bozzo E., Ferraccioli, F. & Wilson T., 1997. Structural Framework of a High-Resolution Aeromagnetic Survey, Southwestern Ross Sea (Antarctica). *Terra Antartica*, **4**(1), 51-56.

Cape Roberts Science Team, 1998. Initial Report on CRP-1, Cape Roberts Project, Antarctica. *Terra Antartica*, **5**(1), 187 p.

Davey F.J. & Brancolini G., 1995. The Late Mesozoic and Cenozoic structural setting of the Ross Sea region. In: Cooper A.K., Barker P.F. & Brancolini G. (eds.), *Geology and Seismic Stratigraphy of the Antarctic Margin, Antarctic Research Series*, **68**, AGU, Washington, 167-182.

Dyke C.G., 1989. Core disking: its potential as an indicator of principal in-situ stress directions. In: Maury V. & Fourmaintraux D. (eds.), *Rock at Great Depth*, Rotterdam, Balkema, **2**, 1057-1064.

Engelder T., 1987. Joints and shear fractures in rock. In: Atkinson B. (ed.), *Fracture Mechanics of Rock*, Academic Press, London, 27-69.

Evans M.A., 1994. Joints and décollement zones in Middle Devonian shales: Evidence for multiple deformation events in the central Appalachian Plateau. *Geological Society of America Bulletin*, **106**, 447-460.

Kleinspehn K.L., Pershing J. & Teyssier C., 1989. Palaeostress stratigraphy: A new technique for analyzing tectonic control on sedimentary-basin subsidence. *Geology*, **17**, 253-256.

Krantz R.W., 1988. Multiple fault sets and three-dimensional strain: theory and application. *Journal of Structural Geology*, **10**, 225-237.

Kulander B.R., Barton C.C. & Dean S.L., 1979. The application of fractography to core and outcrop investigations. *Technical report for the U.S. Department of Energy,* Contract EY-77-Y-21-1321, METC/SP-79/3, 174 p.

Kulander B.R., Dean S.L. & Ward B.J. Jr., 1990. Fractured Core Analysis: Interpretation, Logging, and Use of Natural and Induced Fractures in Core. *American Association of Petroleum Geologists Methods in Exploration Series*, **8**, 88 p.

Li Y. & Schmitt R., 1997. Well-bore bottom stress concentration and induced core fractures. *American Association of Petroleum Geologists Bulletin*, **81**, 1909-1925.

Lorenz J.C., Finley S.J. & Warpinski N.R., 1990. Significance of coring-induced fractures in Mesaverde core, northwestern Colorado. *Amer. Assoc. of Petroleum Geologists Bull.*, **74**, 1017-1029.

Obert L. & Stephenson D.E., 1965. Stress conditions under which core disking occurs. *Society of Mining Engineers Transactions*, **232**, 227-235.

Plumb R.A. & Cox J., 1987. Stress directions in eastern North America determined to 4.5 km from borehole elongation measurements. *Journal of Geophysical Research*, **92**, 4805-4816.

Reches Z., 1978. Analysis of faulting in three-dimensional strain field. *Tectonophysics*, **47**, 109-129.

Salvini F., Brancolini G., Busetti M., Storti F., Mazzarini F. & Coren F., 1997. Cenozoic geodynamics of the Ross Sea region, Antarctica: Crustal extension, intraplate strike-slip faulting, and tectonic inheritance. *Journal of Geophysical Research*, **102**, 24669-24296.

Tessensohn F. & Worner G., 1991. The Ross Sea rift system, Antarctica: structure, evolution and analogues. In: Thomson M.R.A., Crame J.A. & Thomson J.W. (eds.), *Geological Evolution of Antarctica*, Cambridge University Press, Cambridge, 273-277.

Teyssier C., Kleinspehn K. & Pershing J., 1995. Analysis of fault populations in western Spitsbergen: Implications for deformation partitioning along transform margins. *Geological Society of America Bulletin*, **107**, 68-82.

van der Wateren F.M., 1987. Structural geology and sedimentology of the Dammer Berge push moraine, FRG. In: van der Meer J.J.M. (ed.), *Tills and Glaciotectonics*, Balkema, Rotterdam, 157-182.

van der Wateren F.M., 1995. Structural geology and sedimentology of push moraines - processes of soft sediment deformation in a glacial environment and the distribution of glaciotectonic cycles. *Mededelingen Rijks Geologische Dienst*, **54**, 1-168.

Wilson T.J., 1992. Mesozoic and Cenozoic kinematic evolution of the Transantarctic Mountains. In: Yoshida Y., Kaminuma K. & Shiraishi K. (eds.), *Recent Progress in Antarctic Earth Science*, Terra Sci., Tokyo, 303-314.

Wilson T.J., 1995. Cenozoic transtension along the Transantarctic Mountains-West Antarctic rift boundary, Southern Victoria Land, Antarctica. *Tectonics*, **14**, 531-545.